

Intermittent transient chaos at interior crises in the diode resonator

R. W. Rollins and E. R. Hunt

Department of Physics and Astronomy, Ohio University, Athens, Ohio 45701

(Received 23 January 1984)

We report experimental measurements and calculations using a model on a driven, dissipative, dynamical system which shows chaotic behavior. The system is the diode resonator composed of the series combination of a generator, inductor, and a p - n -junction diode. It is studied where there are sudden transient changes in the strange attractor, phenomena called crises by Grebogi, Ott, and Yorke, for which a universal scaling law exists. We verify the scaling law both experimentally and with model calculations. Furthermore, the Lyapunov exponent, a measure of sensitivity to initial conditions, is shown by both methods to increase rapidly but continuously through the crisis region.

GENERAL INTRODUCTION

The motion of driven nonlinear dissipative physical systems is often observed to settle into a state of sustained nonperiodic turbulent or chaotic behavior. It has been found that many of these systems show patterned routes to chaos which are well described by the universal behavior of iterated, unimodal, one-dimensional maps.¹ Also, many features of the chaotic behavior of these systems are surprisingly well described by simple one-dimensional maps. We report here the experimental observation of a "universal" scaling law in the chaotic behavior of the p - n -junction diode resonator in the vicinity of interior crisis.^{2,3} We discuss the behavior in terms of the exact one-dimensional mapping function which we have recently obtained from a model of the p - n -junction diode⁴ and in terms of an extension of that model to two dimensions.⁵ We also report values of the Lyapunov exponent, which gives a measure of the predictability for the system, in the neighborhood of interior crisis.

Recently, Grebogi, Ott, and Yorke^{2,3} have discussed the occurrence of sudden qualitative changes in the chaotic dynamics of nonlinear systems in terms of one- and two-dimensional quadratic maps. These changes occur at particular values of the "drive" parameter, where an unstable periodic orbit enters the region of phase space occupied by the orbit of the sustained chaotic state into which the system settles. The region of phase space into which the system settles is called an *attractor* and Grebogi, Ott, and Yorke have assigned the term *crisis* to the phenomenon of the joining of the unstable orbit with the attractor. Recent reports^{6,7} of experimental observations of the driven nonlinear p - n -junction diode resonator show the qualitative changes in the attractor at crisis as described by Grebogi, Ott, and Yorke. In this paper we report both measurements and model calculations for the p - n -junction diode-resonator system which show the onset of intermittent, transient, chaotic behavior of the response as the amplitude of the drive voltage is increased beyond the critical value where crisis occurs.

QUANTITATIVE DESCRIPTION OF CRISIS

The response of a driven anharmonic p - n -junction diode resonator, composed of a resistance, inductance, and a diode in series with an oscillator, has been found to exhibit a pattern of period doubling^{8,9} and tangent-bifurcation-intermittency¹⁰ routes to chaos, in good agreement with universal behavior found in iterated one-dimensional maps. We have shown that a simple, piecewise linear model of the diode, which characterizes the p - n -junction by a forward bias voltage, reverse capacitance, and reverse recovery time, reduces exactly to a one-dimensional map over a range of circuit parameters and drive voltages.⁴ The map is of the form

$$|I_m|_n \rightarrow |I_m|_{n+1} = F_1(|I_m|_n; V), \quad (1)$$

where $|I_m|_n$ is the maximum forward current through the p - n -junction during the n th cycle, V is the magnitude of the drive voltage, and the mapping function F_1 is given by the step-by-step procedure described in Ref. 4. We chose a very simple function to characterize the reverse recovery time for the n th cycle: $\tau_{r,n} = f(|I_m|_n)$, where $f(I) = \tau_m [1 - \exp(-I/I_c)]$; τ_m and I_c are parameters characterizing the particular p - n -junction used. Recently, we have shown that the reverse recovery time depends not only on the last conducting cycle but on the conducting cycle previous to that as well. Thus, we extended the model to include this characteristic⁵ by choosing $\tau_{r,n} = f(|I_m|_n) + \alpha f(|I_m|_{n-1})$, where α is a parameter. For $\alpha = 0$ we have the previous model, Eq. (1), and $\alpha \neq 0$ leads to a two-dimensional map of the form

$$|I_m|_{n+1} = F_2(|I_m|_n, |I_m|_{n-1}; V) \quad (2)$$

over a range of circuit parameters and drive voltages. Iteration of this map with $\alpha \neq 0$ has been shown to yield an attractor with the qualitative features of a corresponding attractor measured on a p - n -junction diode resonator.⁵ The calculations reported here use this model.

For the most part, we report calculations and measure-

ments taken with the drive parameter above the stable period-3 window and in the neighborhood of the crisis value V_{3c} . (This point corresponds to $C = C_{*3}$, as shown in Fig. 2 of Ref. 2, using their notation, and to point *B* in Fig. 2 of Ref. 6.) Precisely at $V = V_{3c}$ the unstable period-3 orbit, created together with the stable orbit at the period-3 tangent-bifurcation point, coincides with one end of each of the three bands of the chaotic attractor. (The chaotic attractor forms above $V = V_{3\infty}$, where $V_{3\infty}$ is the accumulation point for period-doubling bifurcations of the original period-3 stable orbit.) The point where $V = V_{3c}$ is called interior crisis by Grebogi, Ott, and Yorke. As V increases beyond V_{3c} the attractor suddenly (discontinuously) expands to include the regions between the period-3 bands. Grebogi, Ott, and Yorke distinguish between "interior crisis," which we are discussing in this paper, the "boundary crisis" where the domain of attraction for one attractor disappears and another attractor appears.

The behavior of the *p-n*-junction diode-resonator system near this interior crisis point is best understood by consideration of the third iterate of the model mapping function of Eq. (1),

$$|I_m|_{n+3} = F_1^{(3)}(|I_m|_n; V),$$

where $F^{(3)}(I) = F(F(F(I)))$. The third iterate is shown in Fig. 1. We have used the one-dimensional model here for clarity in describing the essential features of the behavior of the system at, or near, crisis. The reduced circuit parameters used for this calculation listed in the figure caption are not critical and were chosen to be the same order of magnitude as those of our physical circuit.

The solid line in Fig. 1 is the calculated third-iterate mapping function, while the points (plus signs) show 256 successive iterates after an initial 744 iterates of F_1 . The pattern shown by the points is independent of the starting value of $|I_m|$ and represents the attractor for the particular value of the drive voltage. The intersection of the 45-deg line and the third-iterate mapping function (inside the circles in Fig. 1) gives the unstable fixed points I_u for the third iterate. As the drive voltage is increased from a value below V_{3c} [Fig. 1(a)], to a value above V_{3c} [Fig. 1(b)], the chaotic bands of the attractor increase in length until the unstable fixed point I_u is included in the attractor. This first occurs at $V = V_{3c}$.

Figure 2 is an expanded view of the upper right-hand portion of Fig. 1(b), including one of the chaotic bands. Iteration of the map shown in Fig. 2 shows that the system remains trapped in the chaotic band until it "happens" to visit the region near I_u but below the 45-deg line. It then "escapes" the chaotic band and will wander wildly over the rest of the third-iterate mapping function until the forward current peak happens to fall within a band again. Once the system is within a chaotic band it can escape only through the small "exit" region near I_u , as described above. Hence, when $V > V_{3c}$, the attractor consists of two distinct parts: the "chaotic trap" region and the "intermediate" region. The chaotic trap region is composed of three bands, which were the entire attractor before crisis, and above crisis act as a trap with a small but finite escape probability. The intermediate region is the

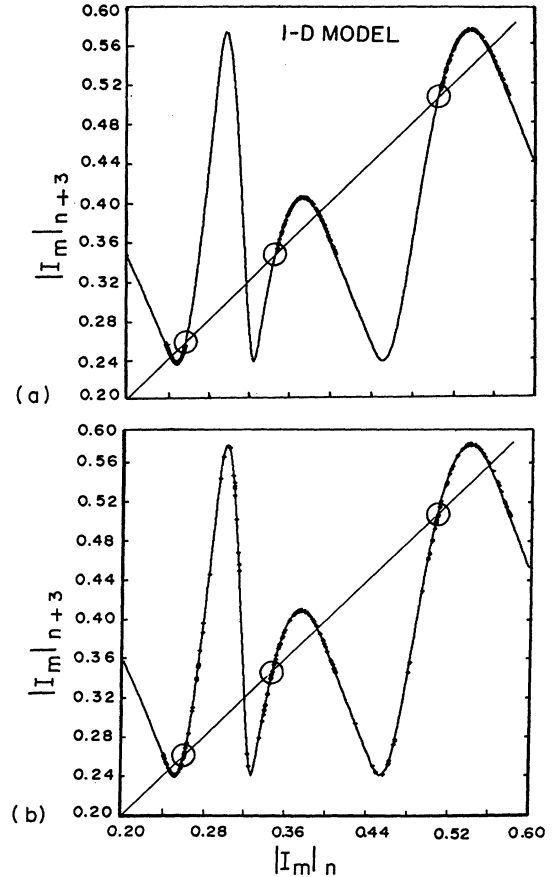


FIG. 1. The solid line is the third iterate of the mapping function F_1 obtained from the one-dimensional model. The points are $|I_m|_{n+3}$ vs $|I_m|_n$ (in units of V_f/R) for the 734th through the 990th cycle and represent the attractor. (a) $V/V_f = 12.40$ and below crisis. (b) $V/V_f = 12.60$ and above crisis. In both cases, the circuit parameters were $\omega = \omega_0$, $Q = 15$, $\tau_m \omega_0 / 2\pi = 1$, and $I_c R / V_f = 2.0$ using the notation of Ref. 4. The unstable fixed points I_u are within the circles at the intersection of the 45-deg line and the third iterate of F_1 .

region between the bands where the system is rarely found, because once having escaped from the trapping portion of the attractor the system is quickly trapped again.

For $V > V_{3c}$, the system intermittently escapes from and becomes trapped in the period-3 chaotic bands. We describe the dynamical behavior of the system quantitatively by defining the following quantities. Each time the system is trapped in a period-3 band, we refer to it as an "event." The system is observed for a period of time during which there are a total of N_T trapping events and on the i th event the system remained trapped for L_i threefold iterates. The probability of being trapped for L threefold iterates is $P(L) = N(L) / N_T$, where the distribution function $N(L)$ is the number of times the system remains trapped in the chaotic bands for exactly L threefold iterates and N_T is sufficiently large. The average L for the set of N_T trapping events is $\langle L \rangle = \sum_{L=0}^{\infty} L P(L)$.

Recently, Grebogi, Ott, and York³ indicate that systems described by maps will exhibit universal behavior near internal crisis such that

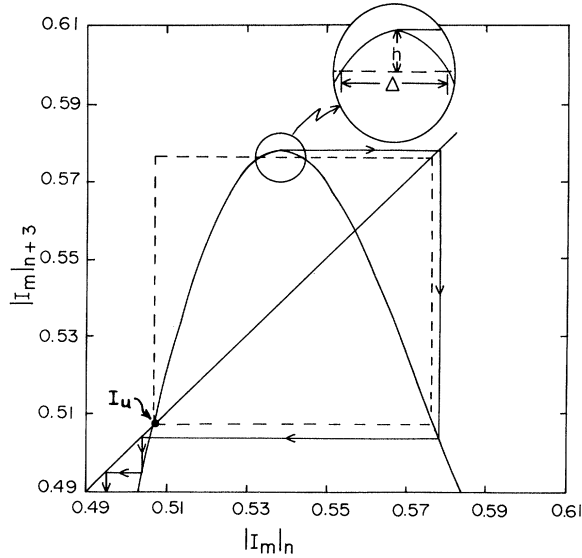


FIG. 2. An expanded view of the upper right-hand part of Fig. 1(b) showing the third iterate of F_1 . Iteration of any point on the map within the dashed box will remain trapped in the region.

$$P(L) = \langle L \rangle^{-1} \exp(-L/\langle L \rangle), \quad (3)$$

and for maps with a quadratic maximum

$$\langle L \rangle \propto \epsilon^{-1/2}, \quad (4)$$

where $\epsilon = (V - V_{3c})/V_{3c} \ll 1$. We arrived independently at the same result by the argument given below, which is similar to theirs.

Tracing the path followed by the iterates on the map shown in Fig. 2 demonstrates that points on the map which are outside the dashed box will escape the period-3 chaotic band. Escape is assured once the peak forward current falls in the region of length Δ near the maximum. Both iteration of the model map and experimental observations reported below (see Fig. 5) show that the distribution of third-iterate current peaks during a trapping event is a smooth, flat function over the region near the maximum. Thus, the assumption of a random distribution of entrance current peaks would allow a statistical treatment of the system. However, this assumption is unnecessarily strong since, as we demonstrate in the next section, the Lyapunov exponent is positive over a range of the drive parameter which includes the crisis point. The sensitive dependence on initial conditions for systems exhibiting chaotic behavior makes the statistical description of a completely deterministic system possible.^{11,12} Thus, any distribution in the entrance current peaks will lead to a neighborhood near the crisis point where the statistical description is valid. The probability that the system will escape on any particular third iterate is q , and we expect q to be proportional to the length of the escape region Δ .

The probability of escape after exactly L threefold iterates is

$$P(L) = q(1-q)^L = q \exp(-\beta L), \quad (5)$$

where $\beta = -\ln(1-q)$. If $V \gtrsim V_{3c}$, then $\epsilon \approx 0$, $q \ll 1$, and

$\beta \approx q$. In this limit the sum for $\langle L \rangle$ may be replaced by an integral,

$$\langle L \rangle = \int_0^\infty Lq \exp(-qL) dL = q^{-1}. \quad (6)$$

Equations (5) and (6) lead to Eq. (3).

The relationship between $\langle L \rangle$ and ϵ depends on the shape of the maximum of the mapping function. As ϵ is increased from zero, the maximum in $F^{(3)}(I)$ moves up through the dashed box shown in Fig. 2. The height h of the maximum above the dashed box is a function of ϵ . The function has the properties $h(\epsilon=0)=0$, $h(\epsilon)<0$ if $\epsilon<0$, and $h(\epsilon)>0$ if $\epsilon>0$. In general, the leading term in an expansion of $h(\epsilon)$ about $\epsilon=0$ will be proportional to ϵ and, thus, the length Δ is proportional to $\epsilon^{1/2}$ if the maximum in $F^{(3)}(I)$ is of order z . The order of the extrema in $F^{(3)}(I)$ is the same as the order of the extremum in $F(I)$. Therefore, if $F(I)$ has an extremum of order z , then $q \propto \epsilon^{1/z}$ and Eq. (6) gives

$$\langle L \rangle \propto \epsilon^{-1/z}, \quad (7)$$

since $q \propto \Delta$. Equation (7) reduces to Eq. (4) for a quadratic extremum where $z=2$.

In general, behavior near internal crisis associated with a period- n window may be similarly described by consideration of the n th iterate of the map. Hence, the results above are of universal validity for one-dimensional maps.

EXPERIMENTAL RESULTS

The physical diode resonator is composed of the series combination of a diode, an inductor, and a signal generator. Also included in the series loop is an operational amplifier used as a current-to-voltage converter. The diode we use is a Westinghouse 1N1211 rectifier—a Si p - n - j junction, but any diode with a recovery time comparable to the drive period will suffice. At sufficiently low drive voltages the inductor (14 mH, 80 Ω at 100 kHz) resonates with the diode capacity at approximately 100 kHz. It was found necessary to filter the output of our signal generator using a bandpass filter to remove spurious amplitude modulation. The output of the bandpass filter drives the resonator circuit through another operational amplifier to reduce the drive impedance to practically zero. The resulting drive signal has an amplitude modulation and drift of less than 1 part in 5000. The frequency used was 80 kHz and found not to be critical.

Figure 3 shows the third iterate of the map with the drive voltage just above the period-3 crisis ($\epsilon=0.01$). The forward currents on the n th and $n+3$ rd cycles are peak detected and held for several cycles and displayed on the x and y axes of an oscilloscope. The brighter lines indicate the points which are also visited in the chaotic period-3 region just below crisis. The folding in the lower noisy region is a feature of the two-dimensional nature of the diode resonator.⁵

Figure 4 is a digitized (~ 500 points) version of Fig. 3. Every third current maximum is peak detected, digitized, and stored in a computer. The technique allows the observation of the order in which the points are visited. Shown is a trajectory which begins in the lowest region,

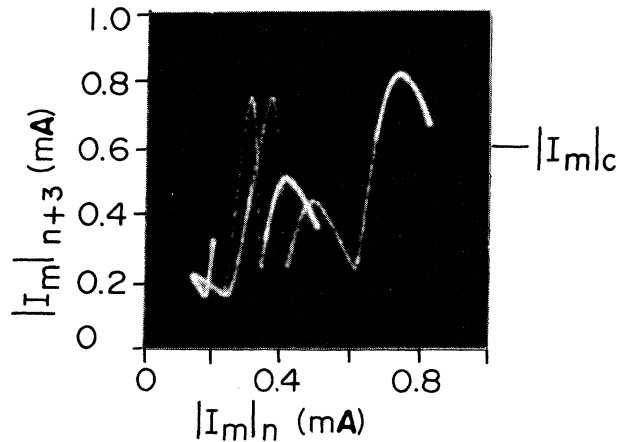


FIG. 3. Third iterate of the map with $\epsilon=0.01$. The three bright areas correspond to the chaotic bands below crisis. The value $|I_m|_c$ is described in the text.

wanders around the map, and eventually is trapped in the upper chaotic region. This is what we call an event, and in this case it lasts five period-3 cycles before the trajectory escapes that region. Experimentally we detect an event by the occurrence of two or more consecutive current peaks, sampled every three drive cycles, larger than the $|I_m|_c$ shown in Fig. 3. The value $|I_m|_c$ is set such that all current peaks in the upper chaotic band trigger a logic circuit which then produces a "true" signal. At least two consecutive current peaks are needed to discriminate against other peaks, shown in Figs. 3 and 4, that are larger than $|I_m|_c$ and are not part of an event.

Figure 5 shows the spectrum of current-peak heights during events. The channel number is linearly related to the current peak with an offset. The drive voltage is just above crisis ($\epsilon=0.0013$). The true signal is applied to the coincidence input of the pulse-height analyzer to discriminate against the unwanted pulses.

The general shape of the spectrum is very similar to that calculated from the logistics equation.¹¹ The two small peaks on the high side of the spectrum correspond to the two most probable entry points. These come from the two peaks in the upper central region of the maps shown in Figs. 3 and 4. The small peak to the left of the

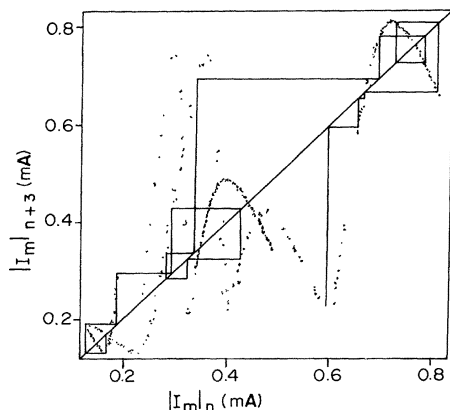


FIG. 4. Digitized version of Fig. 3 showing a trajectory getting trapped in and escaping from the upper chaotic band after five period-3 cycles—an event with $L=5$.

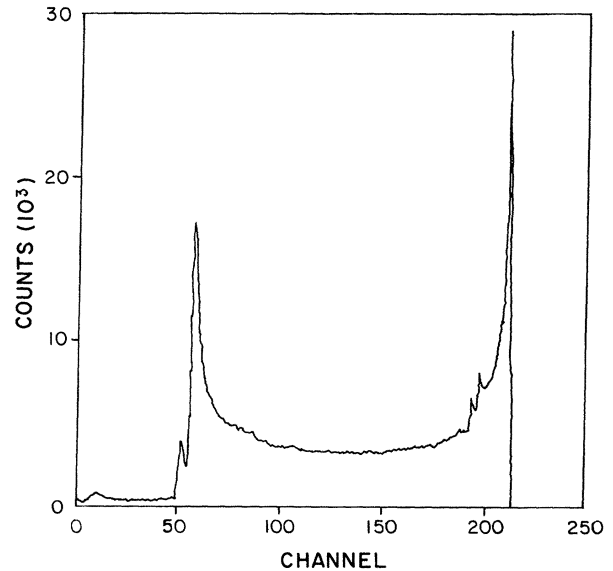


FIG. 5. Spectrum of current-peak heights in the upper chaotic band just above crisis ($\epsilon=0.0013$).

main spectrum corresponds to the first point visited after an event. The central portion of the spectrum is quite flat, justifying our earlier assumption.

Figure 6 shows the number of events of length L occurring out of a total 51 200 events as a function of the length of the orbit for a reduced drive voltage $\epsilon=0.0042$. The data show an exponential decay over 3 orders of magnitude verifying Eq. (5) with the average decay length $\langle L \rangle=19.2$. To obtain these data, pulses representing the current peaks greater than $|I_m|_c$ were counted in a multichannel analyzer. The logic circuit was used to prevent the analyzer from counting except during an event and to advance the channel when the event was over. The number of events for each L was sorted by computer. One

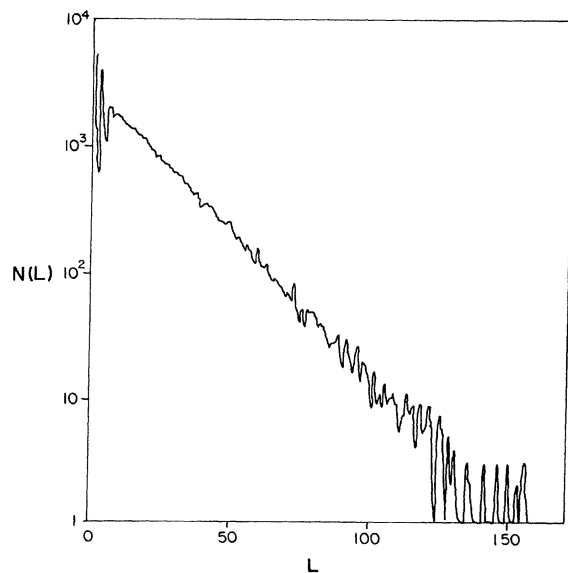


FIG. 6. Number of events of length L as a function of L for $\epsilon=0.0042$. Here $\langle L \rangle=19.2$. The initial transient is discussed in the text.

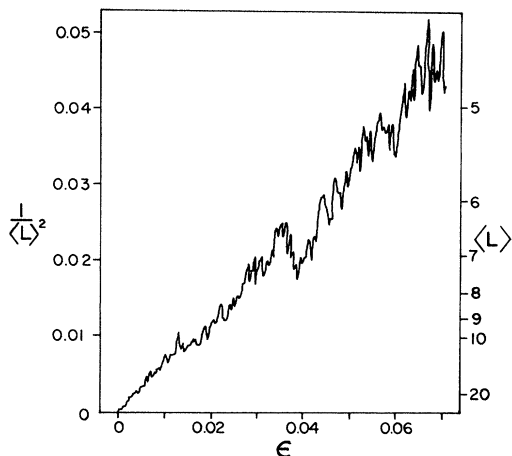


FIG. 7. Average inverse square of L vs ϵ verifying Eq. 7 with $z = 2$.

cause for the initial transient is that the acceptance level of the current peaks $|I_m|_c$ must be adjusted slightly below the upper chaotic region, allowing some peaks from trajectories never actually trapped in the region to be counted. Another cause is the nonrandom distribution of entrance currents which will be discussed in the next section.

The variation of $1/\langle L \rangle^2$ as a function of the reduced

drive voltage ϵ (channel number) is shown in Fig. 7. The average of L is over 1000 events per channel. Over a large range of ϵ and frequency we find Eq. (7) is consistent with our data. For $\epsilon = 0.037$ we observe a reproducible "glitch." We found similar glitches for frequencies between 60 and 100 kHz and with an added 100 Ω series resistance. We believe these glitches are due to a nonrandom entrance distribution.

To obtain these data, we recorded in the multichannel analyzer the number of current pulses greater than $|I_m|_c$ occurring per 1000 events before advancing the channel. The horizontal output of the analyzer (a voltage proportional to the channel number) is used to control the amplitude of the drive voltage, decreasing it by steps occurring with every channel advance. The procedure was to start the system at the highest ϵ desired and allow it to proceed until the crisis point was reached. A computer was used to take $\langle L \rangle$ from the analyzer and compute $1/\langle L \rangle^2$ values for each channel.

The largest Lyapunov exponent λ is a measure of how rapidly nearby points in phase space separate. A negative value of λ corresponds to the system being in a limit cycle, while a positive represents a chaotic or strange attractor. Brandstater *et al.*¹³ have recently determined λ with some confidence in a Couette-Taylor flow experiment. Following their example we digitized (12 bits) 4000 current peaks (which we here call I_i for simplicity) for a

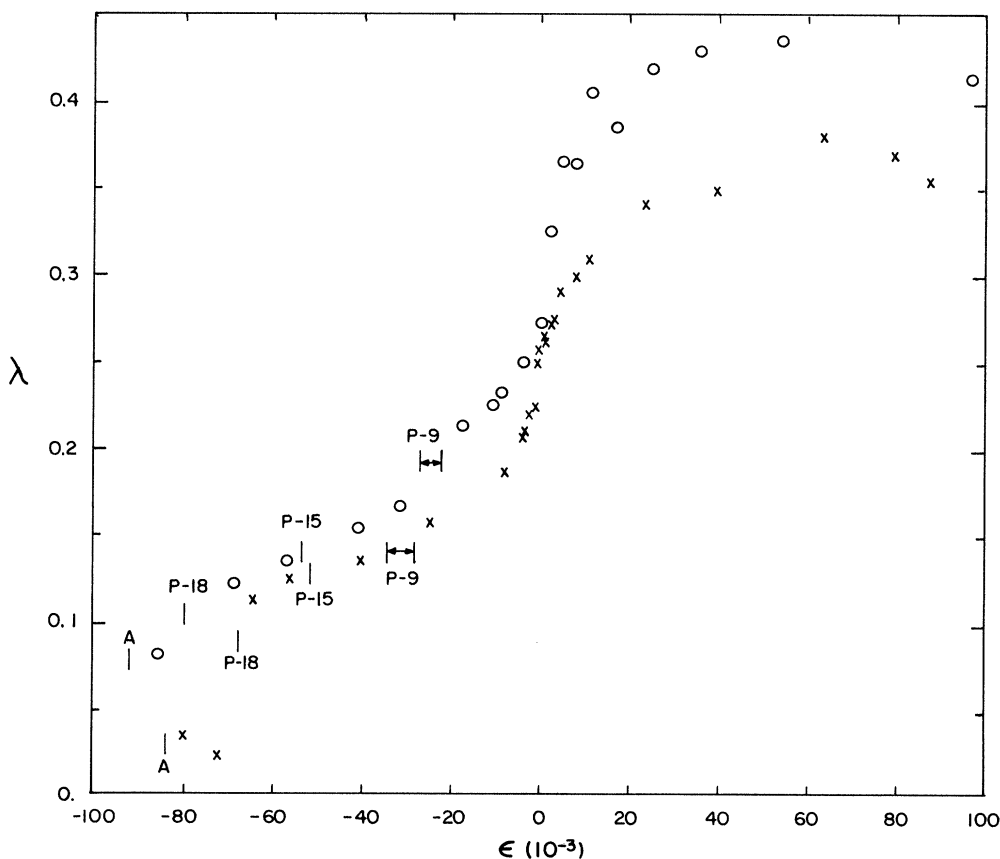


FIG. 8. Lyapunov exponents near crisis. The circles are determined through Eq. (8) by experiment and the crosses from the one-dimensional model through Eq. (9). $P-9$, $P-15$, and $P-18$ are stable orbits of the period indicated, and A is the period-3 accumulation point.

number of values of ϵ and stored the amplitudes in a computer. Using the equation

$$\langle |I_{i+n} - I_{j+n}| / |I_i - I_j| \rangle_{av} = e^{\lambda n}, \quad (8)$$

we determine λ by starting with an arbitrary i and searching the data file to find an I_j very near I_i on the first iterate map. By incrementing n , the separation is then followed until it is no longer small compared with the size of the attractor. Then the second point of the pair I_j is replaced by a new one determined as before. The average is taken over about 400 different values of i . The log of the averaged normalized separations is plotted against n and the slope is determined. A good line is obtained for n between 2 and 10. Since our noise is comparable with the digitizing error (1 bit) and with the initial separation (2 bits), we would expect, and find, larger deviations for $n=1$. Usually, after ten cycles the separation is about 10% of the size of the attractor. The circles in Fig. 8 show the results of these calculations. The regions labeled $P-9$, $P-15$, and $P-18$ are limit cycles with the period indicated and would have a negative Lyapunov exponent. The period-3 accumulation point is denoted by A . The most noteworthy feature is the dramatic but apparently continuous rise at crisis.

MODEL CALCULATIONS

The dynamics of the p - n -junction resonator near crisis was also studied using the two-dimensional model described earlier.⁵ The circuit parameters used were not critical, but again were chosen to be the same order of magnitude as those used in the physical system reported above. For Figs. 9–11, $Q=15$; $\tau_m \omega_0 / 2\pi = 1.2$; RI_c / V_f

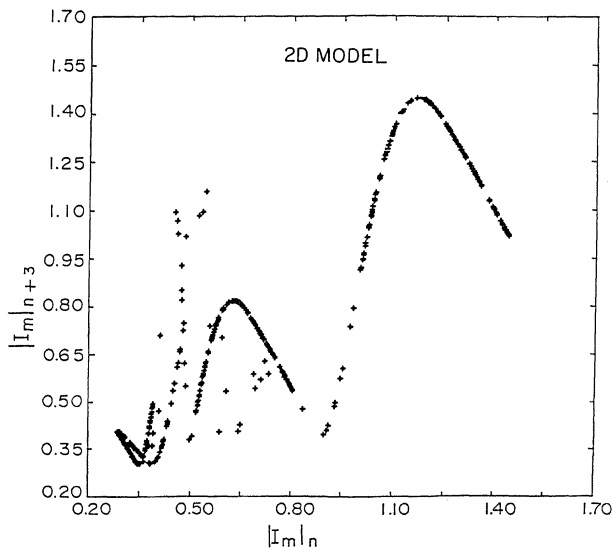


FIG. 9. Third iterates, $|I_m|_{n+3}$ vs $|I_m|_n$ (in units of V_f/R) for the 478th through the 990th cycle using the two-dimensional model with $V/V_f=9.00$ ($\epsilon=0.0136$).

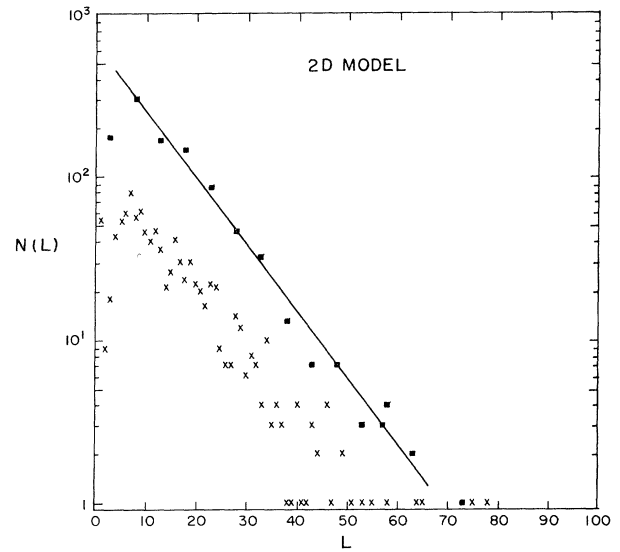


FIG. 10. The number of events of length L as a function of L (x's) using the two-dimensional model with $\epsilon=0.0136$. The boxes are obtained from the same data by summing the events over L in steps of 5 to improve the statistics. The average length of an event is obtained from the slope using Eq. (3) and neglecting the events with small L as discussed in the text. $\langle L \rangle = 10.6$ for the case shown.

$= 2.0$; $\omega = \omega_0$; $\alpha = 0.4$, where $Q = L\omega_0/R$; $\omega_0 = (1/LC)^{1/2}$; and V_f , R , L , and C are the forward bias voltage, resistance, inductance, and reverse capacitance, respectively. We use the same notation here as in Ref. 4. For these values of the circuit parameters, internal crisis above the period-3 window occurs at $V/V_f = 8.87915 \pm 0.00005$, where V is the amplitude of the drive voltage.

Figure 9 is a plot of about 500 third iterates of the forward current peaks with $V/V_f = 9.0$. The model gives very good qualitative agreement with the experimental results displayed in Figs. 3 and 4. The folded, multivalued nature of this attractor is in contrast with the simple at-

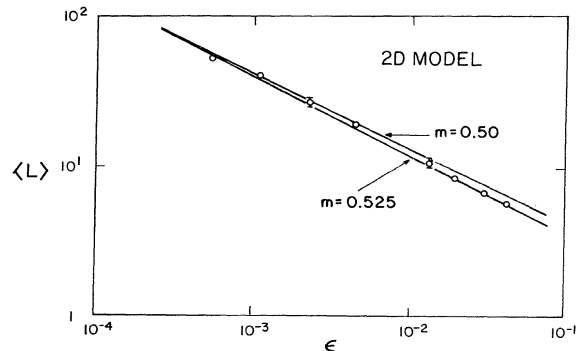


FIG. 11. The average length of an event, $\langle L \rangle$ vs ϵ for the two-dimensional model. The line with slope 0.5 is the universal scaling law of Eq. (7) with $z=2$.

tractor obtained from the one-dimensional model shown in Fig. 1(b).

Figure 10 shows the distribution of the number of trapping events of length L out of a total of 1000 events for $V/V_f=9.0$. The two-dimensional mapping function F_2 was iterated 51 540 times in order to collect these data. Such a calculation required about 40 min of IBM 4341 computer CPU (central processing unit) time. The x 's in Fig. 10 represent the number of events which were observed for each value of L . The squares were obtained from the same data by summing the number of events with length from 1 to 5, 6 to 10, 11 to 15, etc. This was done to improve the statistics and facilitate the taking of slopes to obtain $\langle L \rangle$. These results compare well with the experimental results shown in Fig. 6.

We find that both the experimental results and the model calculations are in good agreement with the exponential form of Eq. (3) for $L \gtrsim L_{\min}$, where $L_{\min} \lesssim 10$. However, for $L \lesssim L_{\min}$, deviations which are clearly beyond statistical fluctuations are observed in both cases. These deviations are, in part, due to the fact that the assumption of a random distribution of entrance currents, used to obtain Eq. (3), is not valid. The distribution of entrance currents is determined by the shape of the attractor at points away from the three chaotic bands. Consideration of Figs. 3 and 4 show that entrance into the upper chaotic band is gained from the two peaks in the attractor which occur at low $|I_m|_n$. The distribution of entrance currents tends to peak at these two maxima. This is a clear violation of an assumption of a random distribution of entrance-current values. The effect which this has on the distribution $N(L)$ for low L depends on the values of the first few iterates of the most probable entrance current. If the first few iterates do not fall in the region of length Δ (see Fig. 2) near the maximum where escape is assured, then $N(L)$, at small L , will be much smaller than Eq. (3) would predict. This is the case in Fig. 10.

For $L \gtrsim L_{\min}$ the distribution behaves as if the dynamics were statistical even though the entrance points are not random. This is due to the sensitive dependence on initial conditions which is indicated by the positive Lyapunov exponent for the attractor. Nearby points separate exponentially, and after L_{\min} iterates, the particular value of the entrance current becomes unimportant. L_{\min} decreases as the Lyapunov exponent increases.

The average length of a trapping event $\langle L \rangle$ was obtained for several values of the drive parameter V by taking the slope of the semi-log plot of the number of events versus L as indicated in Fig. 10. The values of $\langle L \rangle$ are plotted versus ϵ in Fig. 11. The statistical theory [Eq. (7)] predicts a scaling law with $m=0.5$ if the map has a quadratic extrema. Our results are consistent with $m=0.5$ at small ϵ . If all the data are considered, then a slightly larger $m=0.525$ fits the data better. This may indicate a deviation of the calculated results for the larger values of ϵ from the prediction of Eq. (7), which is only valid for $\epsilon \ll 1$.

Finally, the Lyapunov exponent λ was calculated for the 1D model [Eq. (7)] as the drive parameter was increased through crisis. The Lyapunov exponent for a one-dimensional map^{11,14} may be expressed as

$$\lambda = \lim_{N \rightarrow \infty} \frac{1}{N} \sum_{i=1}^N \ln \left| \frac{dF_1(x_i)}{dx} \right|, \quad (9)$$

where dF_1/dx is evaluated at the i th iterate x_i . Since F_1 obtained from the model is not an analytic function, it was necessary to use a numerical method to find the derivative of F_1 at each iterate. We used a simple four-point "extrapolation-to-the-limit" technique.¹⁵ Values of λ were obtained using Eq. (9), truncating the limit at $N=4000$. The results are plotted as x 's in Fig. 8. Different starting values of the current gave the same value of λ to within the size of the points on Fig. 8. Negative values of λ were obtained from Eq. (9) when the drive parameter was within a window of a periodic orbit. For a one-dimensional map, periodic windows exist at every degree of resolution in the drive parameter in the chaotic region. This leads to an infinite number of very narrow negative spikes in the λ versus drive-parameter curve.¹³ However, the width of the periodic window decreases rapidly with increasing periodicity, and, on the scale of Fig. 8, only the periodic windows indicated were observed. Experimental noise is also known to smooth the λ curve.¹⁴ The Lyapunov exponent of the 1D model agrees well with the largest Lyapunov exponent calculated from measurements on the physical system. Both show a sharp but continuous (to within the precision of the calculations) rise as the drive parameter is increased through the crisis point.

CONCLUSIONS

In summary, we have used both experimental measurements and a mathematical model, which leads to a one- or two-dimensional map, to study the dynamics of the p - n -junction diode resonator near internal crisis. We have studied extensively the internal crisis which is associated with the stable period-3 window. The attractor of the system, above but near internal crisis, consists of two parts: a chaotic trap region and an intermediate region. The system intermittently escapes from the chaotic trap region into the intermediate region and then quickly becomes trapped again.

A simple statistical argument is given, using the third iterate of the one-dimensional model map, which leads to the predictions of an exponential decay from the trap region and a scaling law indicating the average length of a trapping event is proportional to $\epsilon^{-1/2}$, where the map has an extremum of order z . These predictions are universal for unimodal one-dimensional maps.

Experimental results and two-dimensional model calculations were presented which show that the probability that the system is trapped for L iterates is an exponentially decreasing function of L . Also, the average length of a trapping event $\langle L \rangle$ is found to be proportional to $\epsilon^{-1/2}$. These results are in agreement with the universal predictions for a one-dimensional map with a quadratic extremum. Calculations of the Lyapunov exponent λ , both from experimental results and from the one-dimensional

model map, show a sharp but continuous rise in λ as the drive parameter is increased through the crisis point. This continuous change in the Lyapunov exponent, in spite of the discontinuous change in the attractor, at crisis is similar to the behavior observed at other intermittency points (at tangent-bifurcation points for example¹⁶). We believe that this is the first time these quantities have been reported for a physical system in the vicinity of crisis.

ACKNOWLEDGMENTS

We thank T. Tigner for his assistance in the electronics, especially with the analyzers, and D. Hunt and N. Thangsprasert for assistance in computer programming. We acknowledge the support of the Ohio University Research Committee.

*We prefer *Physica* (Utrecht) to *Phys.* (Utrecht). *Phys.* is the abbr. for *Physics*.

- ¹M. J. Feigenbaum, *J. Stat. Phys.* **19**, 25 (1978); *Physica* (Utrecht) **7D**, 16 (1983); P. Collet and J.-P. Eckmann, *Iterated Maps on the Intervals as Dynamical Systems* (Birkhauser, Boston, 1980); R. M. May, *Nature* (London) **261**, 459 (1976); J.-P. Eckmann, *Rev. Mod. Phys.* **53**, 643 (1981); E. Ott, *ibid.* **53**, 655 (1981); H. L. Swinney, *Physica* (Utrecht) **7D**, 3 (1983); L. Kadanoff, *Phys. Today* **36**, 46 (1983).
- ²C. Grebogi, E. Ott, and J. A. Yorke, *Phys. Rev. Lett.* **48**, 1507 (1982).
- ³C. Grebogi, E. Ott, and J. A. Yorke, *Physica* (Utrecht) **7D**, 181 (1983).
- ⁴R. W. Rollins and E. R. Hunt, *Phys. Rev. Lett.* **49**, 1295 (1982).
- ⁵E. R. Hunt and R. W. Rollins, *Phys. Rev. A* **29**, 1000 (1984).
- ⁶C. Jeffries and J. Perez, *Phys. Rev. A* **27**, 601 (1983).
- ⁷H. Ikezi, J. S. deGrasse, and T. H. Jensen, *Phys. Rev. A* **28**, 1207 (1983).
- ⁸P. S. Lindsay, *Phys. Rev. Lett.* **47**, 1349 (1981).
- ⁹J. Testa, J. Perez, and Jeffries, *Phys. Rev. Lett.* **48**, 714 (1982).
- ¹⁰C. Jeffries and J. Perez, *Phys. Rev. A* **26**, 2117 (1982).
- ¹¹P. Collet and J.-P. Eckmann, *Iterated Maps on the Interval as Dynamical Systems* (Birkhauser, Boston, 1980), pp. 15–21.
- ¹²R. Shaw, *Z. Naturforsch.* **36a**, 80 (1981).
- ¹³A. Brandstater, J. Swift, H. L. Swinney, A. Wolf, J. D. Farmer, E. Jen, and J. P. Crutchfield, *Phys. Rev. Lett.* **51**, 1442 (1983).
- ¹⁴J. P. Crutchfield, J. D. Farmer, and B. A. Huberman, *Phys. Rep.* **92**, 45 (1982).
- ¹⁵J. S. Vandergraft, *Introduction to Numerical Computations* (Academic, New York, 1978), p. 135.
- ¹⁶J. E. Hirsch, B. A. Huberman, and D. J. Scalapino, *Phys. Rev. A* **25**, 519 (1982).

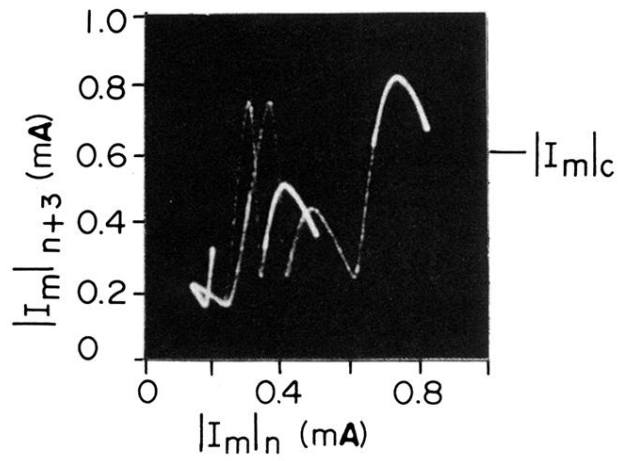


FIG. 3. Third iterate of the map with $\epsilon=0.01$. The three bright areas correspond to the chaotic bands below crisis. The value $|I_m|_c$ is described in the text.